Evaporation of a Sub-Micrometer Droplet

V. Babin*

Institute of Physical Chemistry, Polish Academy of Sciences, Kasprzaka 44/52, 01-224 Warsaw, Poland

R. Holyst

Institute of Physical Chemistry, Polish Academy of Sciences, Kasprzaka 44/52, 01-224 Warsaw, Poland and Department of Mathematics and Natural Science, Cardinal Stefan Wyszyński University, Dewajtis 5, 01-815 Warsaw, Poland

Received: December 12, 2004; In Final Form: April 15, 2005

Evaporation of a spherically symmetric sub-micrometer size liquid droplet is studied using a diffuse interface hydrodynamic model supplemented by the van der Waals equation of state with parameters characteristic for argon. The droplet, surrounded by saturated vapor, is held in a container with the temperature of the walls kept fixed. The evaporation is triggered by a sudden rise of the temperature of the walls. Time and space evolution of the basic thermodynamic quantities is presented. The time and space scales studied range from picoseconds to microseconds and from nanometers to micrometers, respectively. We find that the temperature and chemical potential are both continuous at the interface on the scale larger than the interfacial width. We find that at long times the radius R of the droplet changes with time t as $R^2(t) = R^2(0) - 2t\kappa_v(T_w - T_l)/\ell n_l$, where κ_v is the heat conductivity of the vapor, n_l and T_l are the density and the temperature of liquid inside the droplet, respectively, ℓ is the latent heat of transition per molecule, and T_w is the temperature of the ambient vapor.

I. Introduction

Flows accompanied by evaporation/condensation processes continue to attract much attention because they are ubiquitous in nature and technological applications. Dynamics of such flows is usually modeled in a so-called sharp interface setting.[1] In such an approach, the interface separating liquid/vapor domains is supposed to be infinitely thin. The equations of classical hydrodynamics are then used to describe the motion of each phase separately. The phase transition itself is captured by setting the appropriate boundary conditions on the infinitely sharp interface separating the vapor and the liquid. Different variants of these boundary conditions are employed in the literature. For example, some authors (see, e.g., refs 2 and 3) assume continuity of the temperature across the interface. There is, however, theoretical[4] and experimental[5] evidence that the temperature may be discontinuous; then the interface is characterized by yet another temperature. One more important issue concerns the mass flux across the interface. Often the Hertz-Knudsen formula is employed in this case. It can be obtained using kinetic theory of gases and assuming that the mean free path of molecules in the vapor phase is much larger than the interfacial width.[6] This assumption may not hold if the vapor phase is dense, and different boundary conditions have to be imposed, e.g., the continuity of chemical potential.[7,8]

Despite large progress in the study of the processes at hand there are still several questions that deserve detailed analysis. For example, how do various thermodynamic quantities such as chemical potential, temperature, entropy, etc. change in space and time during evaporation, especially across the interface? Is there any difference between evaporation of large droplets (of centimeter size) and small ones (of micrometer or nanometer size)? Not too far from the liquid/vapor critical point these questions can be addressed efficiently with the use of appropriately combined diffuse interface theory and hydrodynamics.[9−12] In this approach, the interfacial region is represented by continuous variations of density in a way consistent with microscopic theories of the interface.[13] The need for interfacial boundary conditions is thus eliminated.

Although the evaporation/condensation processes have been studied since the end of the 19th century, the phenomenon has not been studied in detail on the mesoscale.[14] In particular, we are unaware of any study of evaporation of a micrometer or sub-micrometer droplet in which the profiles of various thermodynamic quantities are shown in the course of evaporation. It is also unclear how the radius of such droplets changes in the process of evaporation. Recently, evaporation of a thin liquid film has been studied by means of molecular dynamics simulations.[15] These simulations, so far, are restricted to small sizes of the system (below 10 nm) and short times (below 50 ns). Such length and time scales are not easily accessible experimentally. Here we consider spatial and time scales that are larger: from half of a nanometer to a micrometer and from picoseconds to microseconds, respectively. The paper is organized as follows: in the next section we describe the model; in section 3 we apply this model to the problem of evaporation of a droplet of argon. We present numerical solutions of the model equations and discuss obtained results. Conclusions are contained in the last section.

II. The Model

A. Equations of Motion. We used the diffuse interface model coupled with hydrodynamic equations.[10−12,16] In such an approach, the continuous density field varies smoothly in space. High (low) density values correspond to the liquid (vapor) phase. The set of dynamical equations[11] comprises the conservation of mass:

10.1021/jp0443409 CCC: $30.25
Published on Web 05/13/2005

$$\partial_t \rho + \partial_\alpha(\rho u_\alpha) = 0 \tag{1}$$

conservation of momentum:

$$\partial_t(\rho u_\alpha) + \partial_\beta(\rho u_\alpha u_\beta + p\delta_{\alpha\beta} - K\sigma^{(c)}_{\alpha\beta}) = \partial_\beta \sigma^{(v)}_{\alpha\beta} \tag{2}$$

and the equation for the entropy density:

$$T\{\partial_t(\rho s) + \partial_\alpha(u_\alpha \rho s)\} = \sigma^{(v)}_{\alpha\beta}\partial_\alpha u_\beta - \partial_\alpha q_\alpha \tag{3}$$

where ρ is the medium mass density, u_α is the velocity, s is the specific entropy (entropy per unit mass), T is the temperature, p is the thermodynamic pressure, and K is the constant related to the liquid−vapor surface tension. Greek indices label vector and tensor components in Cartesian coordinates and the familiar summation convention $a_\alpha b_\alpha = a_x b_x + a_y b_y + a_z b_z$ is understood. ∂_α stands for $\partial/\partial x_\alpha$ and ∂_t denotes partial derivative with respect to the time t.

The viscous stress tensor $\sigma^{(v)}_{\alpha\beta}$ is supposed to be of the Newtonian form[17] with bulk viscosity set to zero

$$\sigma^{(v)}_{\alpha\beta} = \rho\nu\left(\partial_\alpha u_\beta + \partial_\beta u_\alpha - \frac{2}{3}\delta_{\alpha\beta}\partial_\gamma u_\gamma\right)$$

The heat flux q_α is given by the Fourier Law

$$q_\alpha = -\kappa\partial_\alpha T \qquad \kappa = c_v n \chi \tag{4}$$

In the last formula c_v is the specific heat for constant volume, n is the particle density (i.e., $\rho = mn$, where m is the particle mass). Kinematic viscosity ν as well as thermal diffusivity χ[28] are assumed constant.

Momentum eq 2 coincides with the classical Navier−Stokes equation except for the capillary stress tensor

$$\sigma^{(c)}_{\alpha\beta} = \left(n\nabla^2 n + \frac{1}{2}\left|\nabla n\right|^2\right)\delta_{\alpha\beta} - \partial_\alpha n\, \partial_\beta n \tag{5}$$

which models capillary forces associated with the interface.

For more detailed description of the model interested reader is referred to excellent works.[11,12,18,19]

B. Dimensionless Form. The variables are set to nondimensional form by means of the length δ_L, energy δ_E, temperature δ_T, and time δ_t scales obtained from the critical density n_c (that is, particle density at the critical point), critical temperature T_c, and molecular mass m of the substance:

$$\delta_L = {n_c}^{-1/3} \quad \delta_E = k_B T_c \quad \delta_T = T_c \quad {\delta_t}^2 = \frac{m{\delta_L}^2}{\delta_E} \tag{6}$$

where k_B is the Boltzmann constant. Dimensionless quantities (marked with tildes) can be then related to the physical ones

$$x_\alpha = \delta_L \tilde{x}_\alpha \quad t = \delta_t \tilde{t} \quad \rho = \frac{m}{{\delta_L}^3}\tilde{n} \quad n = \frac{1}{{\delta_L}^3}\tilde{n}$$

$$u_\alpha = \frac{\delta_L}{\delta_t}\tilde{u}_\alpha \quad T = \frac{1}{T_c}\tilde{T} \quad p = \frac{\delta_E}{{\delta_L}^3}\tilde{p} \quad s = \frac{\delta_E}{T_c m}\tilde{s}$$

$$\tilde{K} = \frac{1}{\delta_E {\delta_L}^5}K \quad \tilde{\nu} = \frac{\delta_t}{{\delta_L}^2}\nu \quad \tilde{c}_v = \frac{1}{k_B}c_v \quad \tilde{\chi} = \frac{\delta_t}{{\delta_L}^2}\chi$$

In nondimensional form eqs 1−3 remain unaltered except for the mass density ρ, which is substituted by the dimensionless particle density $\tilde{n}$. Henceforth, we omit the tildes and always use dimensionless quantities unless stated otherwise.

C. Equations of State. The system of eqs 1−3 must be supplemented with two equations of state: $p = p(n, T)$ and $s = s(n, T)$. These can be conveniently obtained from the bulk free energy density $f(n, T)$. We use approximate van der Waals formula, which, for noble gases, reads[20]

$$f(n, T) = nT\ln\frac{n}{3-n} - nT - \frac{9}{8}n^2 - \frac{3}{2}nT\ln\lambda T \tag{7}$$

where

$$\lambda = \left(\frac{1}{3n_c}\right)^{2/3}\frac{mk_B T_c}{2\pi\hbar^2}$$

In the last expression, n_c and T_c are the dimensional critical density and temperature, respectively, and $\hbar$ is the Planck constant.

From eq 7 one readily gets the pressure

$$p = -f + n\left(\frac{\partial f}{\partial n}\right)_T = \frac{3nT}{3-n} - \frac{9}{8}n^2 \tag{8}$$

the entropy density

$$sn = -\left(\frac{\partial f}{\partial T}\right)_n = \frac{5}{2}n + \frac{3}{2}n\ln\lambda T - n\ln\frac{n}{3-n} \tag{9}$$

and the specific heat per molecule at constant volume: $c_v = 3/2$.

For temperature $T = 1 - \delta T$, $\delta T > 0$ below $T_c = 1$, the formula (eq 7) predicts the coexistence of liquid and vapor phases;[20] their densities n_l and n_v can be determined from the requirement of equal pressures and chemical potentials in the two phases. Surface tension of the stationary planar liquid−vapor interface is then given by the following expression[13]

$$\sigma = \sqrt{2K}\int_{n_v}^{n_l} dn\, \sqrt{f(n) - \mu_{eq}n + p_{eq}} \tag{10}$$

where μ_{eq} and p_{eq} are equilibrium values of the chemical potential and pressure correspondingly. For not too large δT the integral in the above formula can be evaluated to give

$$\sigma \approx \sqrt{2K}(\delta T)^{3/2}\left[4 - \frac{82}{125}\delta T - \frac{5533}{61250}(\delta T)^2\right]$$

We have found this approximation to be sufficiently accurate for $\delta T \lesssim 0.4$.

To make a connection with the experiment, we have chosen the material constants corresponding to argon. Physical properties of argon are freely available from the NIST web site.[21] In particular, critical density and critical temperature of argon are

$$n_c = 13407.4\frac{\text{mol}}{\text{m}^3} \quad T_c = 150.687\ \text{K}$$

which gives

$$\delta_L = 4.99 \times 10^{-10} m \quad \delta_t = 2.82 \times 10^{-12} s \quad \lambda = 235.9$$

The remaining parameters can be approximated by the following constant values:

$$K = 1.3 \quad \nu \approx 1 \quad \chi \approx 2$$

We note that the surface tension of the liquid−vapor interface

given by eq 10 agrees quite well with that of argon in wide range of temperatures (from $T \sim 0.6$ up to the narrow critical region near $T_c = 1$, in dimensionless units). On the other hand, neither kinematic viscosity ν nor thermal diffusivity χ of argon are constants. The values chosen provide tolerable approximation in the range of temperatures relevant to our study $0.8 \lesssim T \lesssim 1$.

D. Spherically Symmetric Droplet. Let us turn back to the evaporating liquid droplet. We consider a liquid droplet and saturated vapor in a container with the temperature of the walls of the container, T_w, kept fixed. Initially, the system is in thermodynamic equilibrium. The evaporation is triggered by a sudden increase of T_w. We assume that the system is spherically symmetric and, moreover, that the resulting flow is also spherically symmetric, that is,

$$n = n(r, t) \quad s = s(r, t) \quad u_\alpha = u(r, t)x_\alpha/r$$

where $r^2 = x_\alpha x_\alpha$ is the distance measured from the center of the droplet. The assumption of spherical symmetry is supported by the results of molecular dynamics study of evaporating argon droplet reported in ref 22. In spherical coordinates, the dimensionless equations of motion eqs 1−3 reduce to

$$\partial_t n + \frac{1}{r^2}\partial_r(r^2 nu) = 0 \tag{11}$$

$$\partial_t (nu) + \partial_r\left[nu^2 + p - K\left(n\left\{\partial_r{}^2 n + \frac{2}{r}\partial_r n\right\} - \frac{1}{2}(\partial_r n)^2\right) - \frac{4}{3}\eta\left(\partial_r u - \frac{1}{r}u\right)\right] = -\frac{2}{r}K(\partial_r n)^2 + \frac{4}{r}\eta\left(\partial_r u - \frac{1}{r}u\right) \tag{12}$$

$$\partial_t(ns) + \frac{1}{r^2}\partial_r\left(r^2\left[nsu - \kappa\frac{\partial_r T}{T}\right]\right) = \frac{4}{3}\frac{\eta}{T}\left(\partial_r u - \frac{u}{r}\right)^2 + \kappa\left(\frac{\partial_r T}{T}\right)^2 \tag{13}$$

where $\partial_r = \partial/\partial r$. The container is thus approximated by a sphere of radius L. The walls are thought to be equally preferably wetted by either phase; that is, the Young's angle is $\pi/2$. This condition implies a vanishing normal derivative of the density at the walls[23]

$$\partial_r n|_{r=L} = 0$$

There is no flow of material through the walls; therefore,

$$u|_{r=L} = 0$$

Boundary conditions at the center of the droplet, $r = 0$, follow from the symmetry argument:

$$u|_{r=0} = \partial_r n|_{r=0} = \partial_r s|_{r=0} = 0$$

The equations of motion (eqs 11−13) are then solved numerically using classical finite differences. We use fourth-order accurate discrete approximations for the spatial derivatives and third-order Runge−Kutta scheme for time-marching.[24] Numerical scheme, similar to one used here, is briefly outlined in ref 25. We used spatial grid consisting of 1024 points for $L = 1024$. We have repeated the computations on the twice finer grid and did not found any significant differences.

III. Evolution of Thermodynamic Quantities and Evaporation Time

Initially, the system is at thermodynamic equilibrium: the radial velocity u is zero; the temperature of the walls of the container, T_w, is 0.85 (128 K for argon); the temperature inside the container is constant $T = T_w$. The initial density profile, shown in Figure 1, corresponds to the liquid droplet with $n = n_l \approx 1.81$ of radius ≈ 134 (669 Å for argon) surrounded by the vapor with $n = n_v \approx 0.32$. We suddenly raise the temperature at the walls of the container to $T_w = 0.95$ (143.2 K for argon) and monitor evolution of the system toward a new equilibrium state, which corresponds to a uniform density profile.

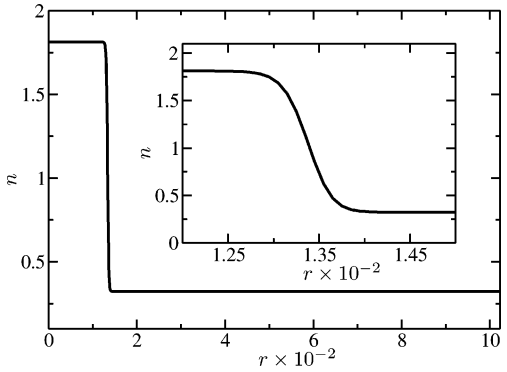

Figure 1. Initial density profile. Interfacial region is shown in the inset. The radial coordinate r and the density n are in units of δ_L and critical density n_c, respectively (for argon $\delta_L = 4.99$ Å).

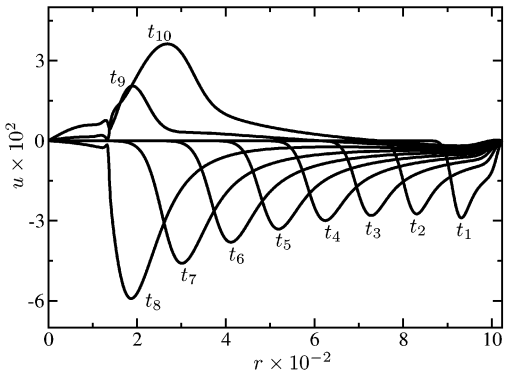

Figure 2. Profiles of the radial velocity u at time $t_1 = 1 \times 10^2$, $t_2 = 2 \times 10^2$, ..., $t_{10} = 1 \times 10^3$ after the wall's temperature has been raised. The wave hits the liquid−vapor interface at time $t_8 < t < t_9$. Reflected wave, propagating in the vapor phase, is clearly visible in the last two snapshots. The time t and the radial coordinate r are in units of δ_t and δ_L, respectively; the velocity u is in units of δ_L/δ_t (for argon $\delta_t = 2.82$ ps and $\delta_L = 4.99$ Å).

Immediately after the increase of the temperature of the walls we observe a wave which moves from the walls toward the droplet. The wave is best visible in the snapshots of the radial velocity, u, shown in Figure 2. When the wave hits the interface, it undergoes partial reflection and excites secondary waves in the liquid phase. The propagation speed of the wave is equal to the speed of sound in the vapor phase; in dimensionless units this speed is close to unity. All thermodynamic quantities exhibit similar behavior. The appearance of these initial waves depends strongly on the dynamics of the heating process. If the temperature of the walls of the container rises gradually, the waves will not be excited.

Later ($t \gtrsim 6 \times 10^4$, corresponding to ≈170 ns for argon), the waves decay and the system enters slow "diffusive" regime, which persists until thermodynamic equilibrium is approached. Finally, the droplet disappears after $t \approx 5.14 \times 10^5$ (for argon $t \approx 1.45$ μs).

In Figures 3−5 the evolution of the density n, temperature T, radial velocity u, chemical potential μ, specific entropy s, and the radial component of the pressure tensor Π_{rr} are

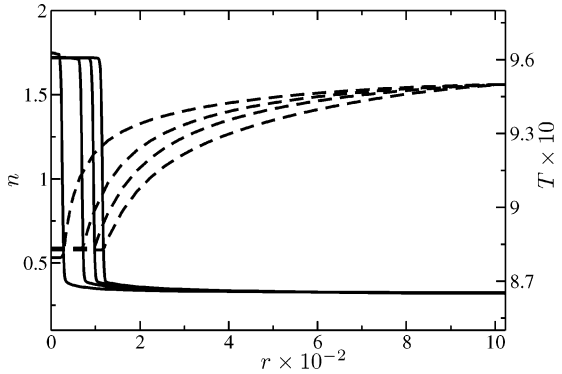

Figure 3. Profiles of the density n (solid line) and temperature T (dashed line) at time $t = 2 \times 10^5$, 3×10^5, 4×10^5, and 5×10^5 after the wall's temperature has been raised. The time t and the radial coordinate r are in units of δ_t and δ_L, respectively; the density n and temperature T are in units of critical density n_c and critical temperature T_c (for argon $\delta_t = 2.82$ ps and $\delta_L = 4.99$ Å).

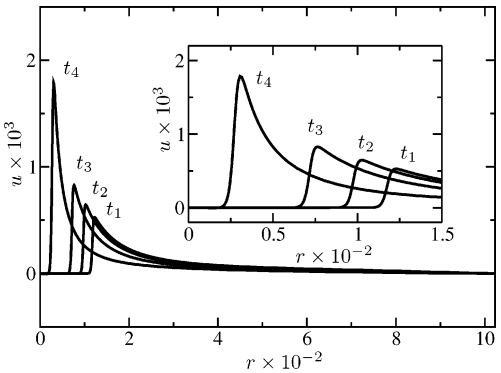

Figure 4. Profiles of the radial velocity u at time $t_1 = 2 \times 10^5$, $t_2 = 3 \times 10^5$, $t_3 = 4 \times 10^5$, and $t_4 = 5 \times 10^5$ after the wall's temperature has been raised. The time t and the radial coordinate r are in units of δ_t and δ_L, respectively; the radial velocity u is in units of δ_L/δ_t (for argon $\delta_t = 2.82$ ps and $\delta_L = 4.99$ Å).

presented. The latter is

$$\Pi_{rr} = p - K\left[n\left(\partial_r^2 n + \frac{2}{r}\partial_r n\right) - \frac{1}{2}(\partial_r n)^2\right] \qquad (14)$$

where thermodynamic pressure p is given in eq 8, and the viscous stress is neglected. The expression for chemical potential, μ, follows from the variational derivative of the square-gradient free energy functional:

$$\mu = -K\nabla^2 n + \left(\frac{\partial f}{\partial n}\right)_T \qquad (15)$$

where f is the free energy density of the uniform system (eq 7).

We define the radius of the droplet, R, as the distance from its center to the inflection point at the interface, that is, position where the sign of the second derivative of the density changes. In Figure 7 we show the time dependence of R. At short times (see inset in this figure), the waves force the volume of the droplet to oscillate (evaporation/condensation and compression/expansion take place). The net effect of this "oscillations stage" is the increase of the droplet size (by a few percent; see Figure 7). Since the liquid density stays almost constant (see Figure 3), the increase of the droplet size is due to the condensation of the vapor. The accompanying release of latent heat in this process heats the droplet. The heating effect depends on the ratio of the latent heat to heat capacity (for argon it is ≈160 K), and, therefore can be quite large. The effect has also been observed in molecular dynamics simulations:[22] very small argon

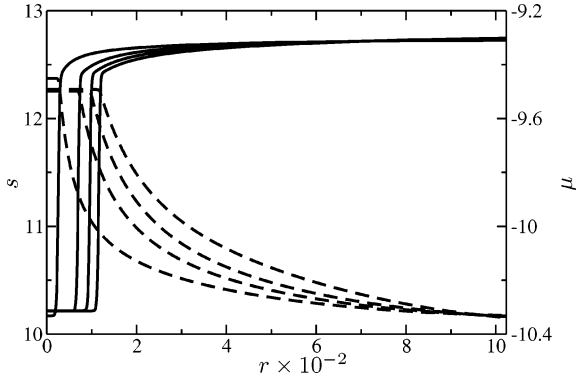

Figure 5. Profiles of the specific entropy s (solid line) and chemical potential μ (dashed line) at time $t = 2 \times 10^5$, 3×10^5, 4×10^5, and 5×10^5 after the wall's temperature has been raised (see eq 15 for the definition of μ). The time t and the radial coordinate r are in units of δ_t and δ_L, respectively (for argon $\delta_t = 2.82$ ps and $\delta_L = 4.99$ Å).

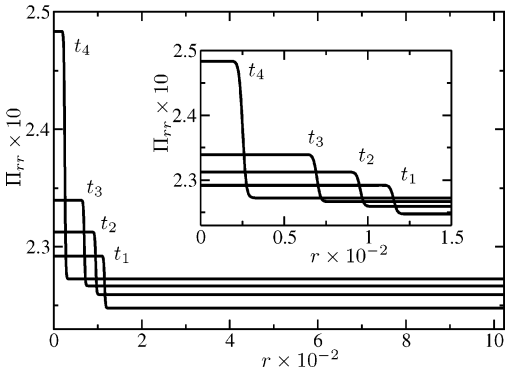

Figure 6. Profiles of the radial pressure Π_{rr} (see eq 14) at time $t_1 = 2 \times 10^5$, $t_2 = 3 \times 10^5$, $t_3 = 4 \times 10^5$, and $t_4 = 5 \times 10^5$ after the wall's temperature has been raised. The time t and the radial coordinate r are in units of δ_t and δ_L, respectively (for argon $\delta_t = 2.82$ ps and $\delta_L = 4.99$ Å).

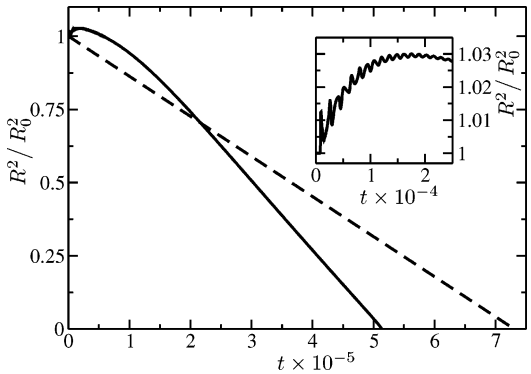

Figure 7. Radius squared (solid line) of the evaporating droplet as function of time; dashed line corresponds to eq 21 with the parameters specified in the text. The radius R and the time t are in units of the initial droplet radius $R_0 = R(t = 0)$ and δ_t respectively (for argon $\delta_t = 2.82$ ps).

droplets initially at 100 K heated to 138 K, when the walls were heated to 300 K. In our case the temperature increased from 128 to 133 K. The oscillation in this initial period of evaporation would also affect the shape of the droplet[26] if we did not restrict it to be spherically symmetric. After this transient behavior the droplet evaporates monotonically with its radius changing according to

$$R \propto (t_0 - t)^{\alpha} \qquad (16)$$

where t_0 is the time when the droplet disappears and $\alpha \approx 1/2$.

We have observed that α depends very weakly (varies by a few percent) on the initial size of the droplet and on the magnitude of the temperature jump. Such dependence is typical for diffusion-limited processes. In our case of strongly first-order phase transition with large latent heat, the heat diffusion is the main limiting factor of the evaporation speed. Moreover, the whole process may be regarded as quasi-stationary (the latter has been pointed out in, e.g., ref 7). The quasi-stationarity is clearly seen in the figures: away from the interface the densities and the pressures of both phases are almost position-independent (mechanical equilibrium); the profile of the temperature T in the vapor phase is very close to the corresponding stationary solution $T \sim T_w - const/r$. The temperature changes noticeably on the scales much larger than the interfacial width. Thus, in the sharp interface limit of the model being used, T should be set continuous across the interface. On the other hand, the density and the velocity are obviously discontinuous in such a limit. The chemical potential μ also varies slowly, and thus it is continuous across the interface in the same limit. The last observation needs a comment. For a one component system at thermodynamic equilibrium, the chemical potential is constant across the system by definition of thermodynamic equilibrium; it can be thus regarded as a function of system's pressure and temperature. In our case of an evaporating droplet, eq 15 defines μ for the system out of equilibrium, under the assumption of local equilibrium. We observed that mechanical equilibrium is established much more quickly than thermal equilibrium. This can be seen, for example, from Figure 6, in which the normal component of the pressure tensor is shown. Indeed, after initial waves have decayed, the pressure became (almost) constant in both phases. Its jump across the interface is $2\sigma/R(t)$ in accordance to the Laplace law. Because the pressure is almost position independent in both phases, the chemical potential changes in space following the temperature profile. Since temperature is continuous across the interface, i.e., changes on a scale much larger than the microscopic size of the interface, so is the chemical potential. The discontinuity of temperature and chemical potential can be expected in the case of a rapid change of pressure around a liquid droplet. Evaporation in the conditions of high vacuum around a liquid droplet would proceed differently from the conditions discussed in this paper. In such a case, there would be no heat flux to the droplet and therefore the droplet will quickly cool. Very low-pressure outside the droplet would preclude the establishment of the mechanical equilibrium.

When the radius, $R(t)$, of the droplet exceeds considerably the width of the interface, the dynamics of the process can be satisfactory explained in the sharp interface setting with the help of a simple energy balance argument (more comprehensive treatment of a similar physical situation can be found in ref 27). The argument is as follows (actually, we proceed along the lines of refs 7 and 8). Since the heat conductivity of the liquid phase is considerably greater than that of vapor, it is reasonable to assume that the temperature inside the droplet, T_l, is spatially uniform. Further, we assume that T_l does not change in time. Both these assumptions are supported by the numerical results. Next, using the observation that the mechanical equilibrium is maintained through the whole process, we assume that the densities of both phases, n_l and n_v, are spatially uniform and time independent, as well. The quasi-stationarity of the process, which is clearly seen from the numerics, can be used to simplify the entropy equation in the region occupied by the vapor phase. Indeed, one arrives at

$$\partial_r(r^2\partial_r T_v) = 0 \tag{17}$$

where the viscous dissipation as well as spatial nonuniformity of the heat conductivity, κ, have been neglected. The profile of the temperature in the vapor phase is then readily obtained from eq 17 using the continuity of the temperature at the interface, i.e., $T_v(r, t)|_{r=R(t)} = T_l$

$$T_v(r, t) = T_w - (T_w - T_l)\frac{R(t)}{r} \tag{18}$$

where the wall of the container has been put at $r = \infty$ for brevity. The evaporation rate per unit area at the interface is

$$\Gamma = n_l[u_l - \partial_t R(t)] = n_v[u_v - \partial_t R(t)] \approx -n_l\partial_t R(t) \tag{19}$$

where u_l and u_v are the radial velocities of the liquid and vapor at the interface, respectively; the last approximation is due to the inequality $n_v u_v \gg n_l u_l$. The energy balance at the interface equates the latent heat consumed per unit area per unit time to the energy dissipated per unit area per unit time

$$\mathcal{L}\Gamma = \kappa\partial_r T_v(r, t)|_{r=R(t)} \tag{20}$$

where $\mathcal{L}$ is the latent heat per particle. The viscous dissipation as well as the kinetic energy of the liquid/vapor both have been omitted in eq 20; it is supported by the numerical results. Finally, combining eqs 18−20, one obtains

$$R^2(t) = R^2|_{t=0} - t\frac{2\kappa_v}{\mathcal{L}n_l}(T_w - T_l) \tag{21}$$

where κ_v denotes the value of the heat conductivity at the vapor side of the interface; that is, $\kappa_v = \kappa|_{n=n_v, T=T_l}$. The numerically obtained time dependence of the radius of the droplet (see Figure 7) agrees qualitatively with that given by eq 21, except for the initial transient period. The amount of time required for the complete evaporation of the droplet can be obtained from eq 21, too. Indeed, the latent heat is readily determined from eq 9 $\mathcal{L} = T_l(s(n_v, T_l) - s(n_l, T_l))$, and the heat conductivity is given by eq 4. For the parameters used in the numerical simulation ($n_l = 1.81$, $n_v = 0.31$, $T_l = 0.85$, and $T_w = 0.95$), eq 21 predicts that the droplet would disappear after $\approx 7.3 \times 10^5$, which is close to the actual value of $\approx 5.14 \times 10^5$.

IV. Summary

In this paper, we have addressed the process of evaporation of a spherically symmetric liquid droplet using a diffuse interface approach coupled to hydrodynamics. We have presented the time evolution of the basic thermodynamic quantities characterizing the system, that is, temperature, density, entropy, pressure, and chemical potential. We have found that the temperature and chemical potential are both continuous at the interface on the scale larger than the interfacial width. The latter observation may be useful for the sharp interface description. The time dependence of the radius of the droplet $R \simeq \sqrt{t_0 - t}$, obtained here for sub-micrometer droplets, agrees with that expected for large droplets; in our case, it is due to the heat diffusion and can be explained using a simple energy balance argument.

A very similar behavior of the temperature and radius of droplet has been observed in microscopic (molecular dynamics) simulations.[22] The approximate formula seems to work relatively well also in that case, i.e., for the droplets of 8 nm radius and wall temperature jumps of the order of 200 K. As we have already discussed, the simple description given by eq 21 breaks

down for the evaporation in a vacuum, i.e., without a heat transfer from the walls. In this case, the droplet would probably cool rapidly. Very low pressure outside the droplet would preclude the establishment of mechanical equilibrium. However, the energy balance would still be applicable, i.e., the latent heat carried by the evaporation flux would be compensated by a decrease of the temperature of the droplet.

Acknowledgment. The authors are indebted to Dr. Piotr Garstecki for the careful reading of the manuscript and useful comments. This work has been supported by the KBN Grant 2P03B00923 (2002−2004).

References and Notes

(1) Delhaye, J. M. *Int. J. Multiphase Flow* **1974**, *1*, 395−409.
(2) Prosperetti, A.; Plesset, M. S. *Phys. Fluids* **1984**, *27*, 1590−1602.
(3) Higuera, F. J. *Phys. Fluids* **1987**, *30*, 679−686.
(4) Bedeaux, D.; Hermans, L. J. F.; Ytrehus, T. *Physica A* **1990**, *169*, 263−280.
(5) Fang, G.; Ward, C. A. *Phys. Rev. E* **1998**, *59*, 417−428.
(6) Ytrehus, T.; Østmo, S. *Int. J. Multiphase Flow* **1996**, *22*, 133−155.
(7) Turski, L. A.; Langer, J. S. *Phys. Rev. A* **1980**, *22*, 2189−2195.
(8) Venugopalan, R.; Vischer, A. P. *Phys. Rev. E* **1994**, *49*, 5849−5852.
(9) Felderhof, B. U. *Physica* **1970**, *48*, 541−560.
(10) Langer, J. S.; Turski, L. A. *Phys. Rev. A* **1973**, *8*, 3230−3243.
(11) Anderson, D. M.; McFadden, G. B. *A Diffuse-Interface Description of Fluid Systems*; Internal Report 5887; National Institute of Standards and Technology: Gaithersburg, MD, 1996.
(12) Antanovskii, L. K. *Phys. Rev. E* **1996**, *54*, 6285−6290.
(13) Rowlinson, J. S.; Widom, B. *Molecular Theory of Capillarity*; Oxford University Press: Oxford, 1989.
(14) Jamet, D.; Lebaigue, O.; Coutris, N.; Delhaye, J. M. *J. Comput. Phys.* **2001**, *169*, 624−651.
(15) Pan, Y.; Poulikakos, D.; Walther, J.; Yadigaroglu, G. *Int. J. Heat Mass Transfer* **2002**, *45*, 2087−2100.
(16) Hohenberg, P. C.; Halperin, B. I. *Rev. Mod. Phys.* **1977**, *49*, 435−479.
(17) Landau, L. D.; Lifshiz, E. M. *Fluid Mechanics*; Pergamon Press: Oxford, 1987.
(18) Anderson, D. M.; McFadden, G. B.; Wheeler, A. A. *Annu. Rev. Fluid Mech.* **1998**, *30*, 139−165.
(19) Español, P. *J. Chem. Phys.* **2001**, *115*, 5392−5403.
(20) Landau, L. D.; Lifshiz, E. M. *Statistical Physics, Part. 1*; Pergamon Press: Oxford, 1980.
(21) http://webbook.nist.gov/chemistry/fluid/
(22) Walther, J. H.; Koumoutsakos, P. *J. Heat Transfer* **2001**, *123*, 741−748.
(23) Seppecher, P. *Int. J. Eng. Sci* **1996**, *34*, 977−992.
(24) Shu, C. W.; Osher, S. *J. Comput. Phys.* **1988**, *77*, 439−471.
(25) Babin, V.; Hołyst, R. *J. Chem. Phys.* **2005**, *122*, 024713.
(26) Lamb, H. *Hydrodynamics*, 6th ed.; Dover Publications: New York, 1945.
(27) Kozyrev, A. V.; Sitnikov, A. G. *Phys.—Usp.* **2001**, *44*, 725−733.
(28) Strictly speaking, thermal diffusivity (or thermotropic conductivity) is defined in ref 17 using the specific heat at constant pressure $\chi = \kappa/nc_p$.